BMC Cancer

RESEARCH

Open Access

Exploring prognostic precision: a nomogram approach for malignant pleural effusion in lung cancer

Yongjie Jiang[1†], Xin Hu[1†], Yiluo Heibi[2], Hang Wu[1], Taibing Deng[2] and Li Jiang[1*]

Abstract

Background Patients with lung cancer and malignant pleural effusion (MPE) often have poor prognoses. Accurate prognostic tools are needed to guide interventions and improve outcomes.

Methods We retrospectively analyzed clinical and imaging data from MPE patients at two medical centers. A nomogram was developed and externally validated. Clinical and imaging features were refined using least absolute shrinkage and selection operator (LASSO), and independent predictors were identified via multivariate logistic regression. Predictors were integrated into the nomogram, whose predictive performance, calibration, and clinical utility were evaluated using statistical analyses, including receiver operating characteristic (ROC) curves, calibration curves, Hosmer-Lemeshow tests, and decision curve analysis (DCA). Survival curves illustrated prognostic differences among risk groups.

Results The final nomogram included five variables: Lactate Dehydrogenase (LDH) levels in pleural fluid, clarity of pleural effusion, treatment regimen, presence of pericardial effusion, and total volume of pleural effusion. In both cohorts, the nomogram demonstrated strong predictive accuracy (Area Under the Curve (AUC): 0.929 and 0.941, respectively) and excellent calibration (Hosmer-Lemeshow test *p*-values: 0.944 and 0.425, respectively). DCA confirmed the nomogram's clinical utility. Risk stratification revealed significant survival disparities among patients.

Conclusion Our nomogram accurately predicts the prognosis of lung cancer patients with MPE at initial diagnosis, incorporating key variables such as LDH levels in pleural fluid, clarity of pleural effusion, treatment regimen, pericardial effusion, and total volume of pleural effusion. Its robust predictive performance, calibration, and clinical utility support its use in guiding clinical decision-making for this patient population.

Keywords Lung cancer, MPE, Prognosis, Nomogram, Predictive modeling

†Yongjie Jiang and Xin Hu contributed equally to this article.

*Correspondence:
Li Jiang
lanqilily@163.com
[1]Department of Respiratory and Critical Care Medicine, Affiliated Hospital of North Sichuan Medical College, Nanchong, China
[2]Department of Respiratory and Critical Care Medicine, Guang'an People's Hospital, Guang'an, China

© The Author(s) 2025. **Open Access** This article is licensed under a Creative Commons Attribution-NonCommercial-NoDerivatives 4.0 International License, which permits any non-commercial use, sharing, distribution and reproduction in any medium or format, as long as you give appropriate credit to the original author(s) and the source, provide a link to the Creative Commons licence, and indicate if you modified the licensed material. You do not have permission under this licence to share adapted material derived from this article or parts of it. The images or other third party material in this article are included in the article's Creative Commons licence, unless indicated otherwise in a credit line to the material. If material is not included in the article's Creative Commons licence and your intended use is not permitted by statutory regulation or exceeds the permitted use, you will need to obtain permission directly from the copyright holder. To view a copy of this licence, visit http://creativecommons.org/licenses/by-nc-nd/4.0/.

Introduction

Pleural effusion is a common medical condition in China, with primary causes including parapneumonic pleural effusion, pyothorax, malignant pleural effusion, and tuberculous pleural effusion [1]. Among these, malignant pleural effusion poses the most dire prognosis, with patients facing an average survival period of merely 5.49 months. Particularly noteworthy is the even shorter survival duration—averaging 2.37 months—for individuals developing malignant pleural effusion later in the disease course compared to those experiencing concurrent malignant pleural effusion at disease onset [2, 3].

While various malignancies can lead to pleural effusion, lung cancer (37.5%), breast cancer (16.8%), and lymphoma (11.5%) are the most prevalent culprits of malignant effusion [4, 5]. A recent meta-analysis, which included 82 studies with 10,748 patients, identified several important prognostic factors for MPE, including clinical parameters such as stage, distant metastasis, and epidermal growth factor receptor mutation, as well as biological markers like hemoglobin, albumin, C-reactive protein, vascular endothelial growth factor, and pleural effusion parameters such as potential of hydrogen, glucose, and survivin [6]. With the continuous evolution of cancer treatment modalities, the management of patients with advanced lung cancer accompanied by malignant pleural effusion has evolved from conventional methods like surgery, radiotherapy, and chemotherapy to encompass more sophisticated strategies. These include chemotherapy combined with radiotherapy, targeted therapy, combination therapy involving targeted therapy and chemotherapy, next-generation targeted therapy, and immunotherapy [7–9].

These advancements have contributed to the improvement of 5-year survival rates among patients with malignant pleural effusions. Nonetheless, existing studies on the treatment of advanced lung cancer patients with malignant pleural effusion often suffer from small sample sizes and limited efficacy data. Therefore, it is imperative to investigate prognostic factors influencing patients with advanced lung cancer and malignant pleural effusion and develop predictive models.

In light of these challenges, this study aims to explore prognostic factors affecting patients with advanced lung cancer and malignant pleural effusion and to develop predictive models. These models are intended to facilitate early interventions and improve both survival outcomes and quality of life.

Methods

Patients

This study adopted a retrospective approach to gather data from patients undergoing treatment at Affiliated Hospital of North Sichuan Medical College and Guang'an People's Hospital from January 1, 2013, to December 31, 2021. The study included individuals initially diagnosed with lung cancer accompanied by malignant pleural effusion. Diagnostic Criteria: Lung Cancer Diagnosis: Diagnosis was confirmed through histopathological examination, encompassing both non-small cell lung cancer and small cell lung cancer. Malignant Pleural Effusion Diagnosis: The diagnosis coincided with the identification of pleural effusion, confirming its malignant nature through pathological assessment of effusion cells or pleural tissue. Alternatively, the diagnosis was supported by clinical criteria met under the following conditions: (a) Histopathological verification of lung cancer with no plausible alternative explanations for pleural effusion. (b) Confirmed lung cancer accompanied by pleural effusion, with imaging modalities (including Computed Tomography (CT), Positron Emission Tomography-Computed Tomography (PET-CT), Magnetic Resonance Imaging (MRI), or ultrasound) showing indications of pleural nodules, masses, or irregular thickening consistent with imaging attributes of pleural metastasis. Exclusion Criteria: (1) Patients without malignant pleural effusion at the initial lung cancer diagnosis. (2) Presence of other malignant tumors. (3) Patients under 18. (4) Incomplete clinical information. (5) Unfollowable patients. The screening and study flow are detailed in Fig. 1.

Clinical feature selection process

All clinical features were initially included in a LASSO for feature selection. Features with non-zero coefficients identified by LASSO were subsequently incorporated into a multivariate logistic regression model for further refinement. From the logistic regression analysis, only features with $P<0.05$ were retained and used in the development of the models.

Image review and feature extraction

The delineation of the region of interest (ROI) for lung cancer was performed by two physicians using MRIcroGL. Discrepancies during the outlining process were resolved through consultation with a third physician. Subsequently, imaging features were extracted from the outlined ROIs using 3D Slicer, resulting in a total of 1037 features.

In the initial analysis, the Mann-Whitney U test was conducted using Python to analyze the imaging features. Features with a significance level of $P<0.05$ underwent standardization through Z-Score transformation and were subsequently included in Lasso for further screening. This process ultimately identified 10 imaging labels. The radscore score were then computed based on these 10 labels (eTable 1 in the Supplementary materials).

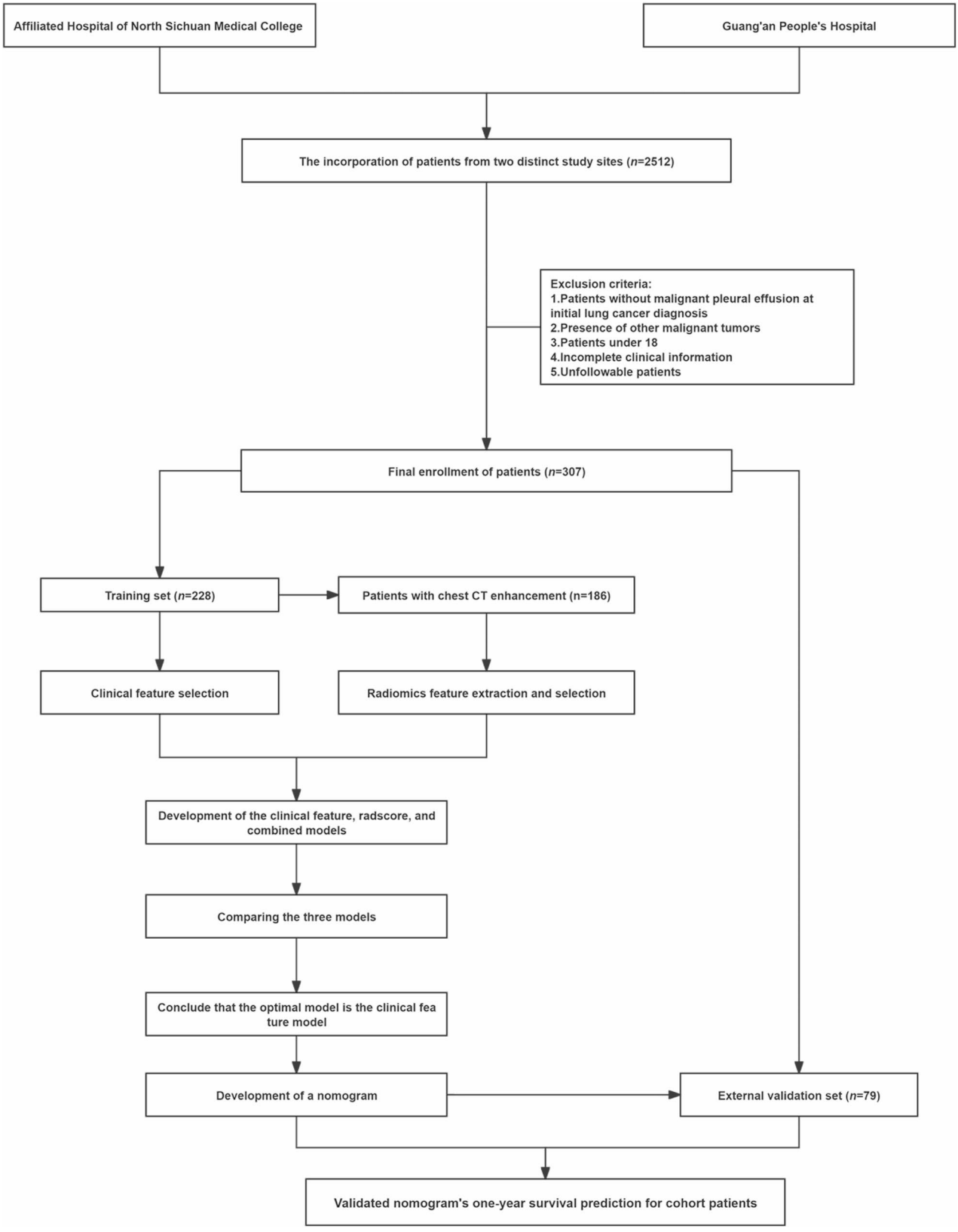

Fig. 1 The comprehensive flowchart, illustrating the process from patient selection to nomogram establishment

Statistical analysis

This study utilized the above features to construct the following three models: the clinical features model, the radscore model, and the combined model. The performance of the models was assessed using ROC curves, and sensitivity, specificity, accuracy, Negative Predictive Value (NPV), and Positive Predictive Value (PPV) were calculated for different models. The DeLong test was used to compare the AUC of different models. The calibration ability of the models was evaluated through calibration curves, which measure the agreement between predicted and observed probabilities. The Hosmer-Lemeshow test was employed to evaluate model fit. The clinical significance of the column charts was assessed using DCA, a statistical methodology used to evaluate the clinical utility of diagnostic and prognostic strategies by demonstrating the net benefit of using the model compared to alternative strategies. Survival curves were utilized to illustrate the prognosis of patients in various risk groups [10]. All statistical analyses mentioned above were performed using R software version 4.1.3.

Results

Analysis and selection of clinical features

After adhering to the inclusion and exclusion criteria, a total of 228 patients were included in the study from Affiliated Hospital of North Sichuan Medical College, constituting the training set (eTable 2 in the Supplementary materials). An additional 79 patients from Guang'an People's Hospital were utilized as the external validation set (eTable 3 in the Supplementary materials). Following screening via Lasso, 17 variables persisted, encompassing parameters such as age, smoking history, pathological subtype of lung cancer, levels of high-sensitivity C-reactive protein in pleural fluid, albumin concentration in pleural fluid, LDH levels in pleural fluid, clarity of pleural effusion, nucleated cell count in pleural fluid, white blood cell count, total volume of pleural effusion, treatment regimen, presence of pericardial effusion, primary tumor site, hypertension, respiratory tract infection, acid-base imbalance, and adrenal metastasis (Fig. 2A and B). Subsequent multifactorial logistic regression analysis identified five variables as the most significant predictors: LDH levels in pleural fluid, clarity of pleural effusion, treatment regimen, presence of pericardial effusion, and total volume of pleural effusion (Fig. 2C). These factors were found to be closely associated with patient prognosis.

Comparison of clinical features model, radscore model, and combined model

We began our analysis with data from 228 patients in the training set, from which we obtained imaging data from chest enhancement CT scans of 186 patients. By analyzing these scans, we extracted a total of 10 radiomic features (eFigure 1, eTable 1 in the Supplementary materials)). With this information from 186 patients, we developed three predictive models: the radscore model, the clinical features model, and the combined model. These models incorporated both screened clinical features and imaging features to predict the 1-year survival of the patients. The radscore model yielded an AUC of 0.694 (95% Confidence Interval (CI): 0.619–0.770), while the clinical features model showed an AUC of 0.937 (95% CI: 0.904–0.970), and the combined model achieved an AUC of 0.951 (95% CI: 0.923–0.980) (Fig. 3A). Notably, the radscore model exhibited the lowest AUC, whereas there was no statistically significant difference between the AUC values of the clinical features model and the combined model ($P = 0.061$). The DCA of the three models indicating that the clinical features model and combined model outperformed the radscore model in terms of clinical efficacy (Fig. 3B). Additionally, calibration curves suggest that the clinical features model and combined model demonstrated the best predictive performance, while the radscore model performed the least accurately (Fig. 3C, D and E).

In summary, owing to its simplicity and ability to maintain prediction accuracy with less clinical information, the clinical features model emerged as the preferred choice. Therefore, we chose to utilize only the five screened clinical features to construct the nomogram.

Development and validation of the nomogram

A nomogram developed from the data of 228 patients in the training set, incorporating five clinical features: LDH levels in pleural fluid, clarity of pleural effusion, total volume of pleural effusion, treatment regimen, and presence of pericardial effusion (Fig. 4A). The ROC curve of the nomogram in the training set shows an AUC of 0.929 (95% CI: 0.897–0.961) (Fig. 4B). Similarly, in the external validation set, the ROC curve of the nomogram demonstrates an AUC of 0.941 (95% CI: 0.885–0.997) (Fig. 4C). Notably, there was no statistically significant difference in the AUC between the training set and the external validation set ($P = 0.711$). Table 1 provides details on sensitivity, specificity, PPV, NPV, and accuracy of the nomogram in both sets, highlighting its commendable discriminative and predictive accuracy. Additionally, in the training set, the calibration curves of the nomogram demonstrate a close alignment of the predicted probability with the actual probability, confirming the model's predictive performance (Fig. 4D). In the external validation set, despite slight fluctuations in the calibration curves of the nomogram, they still remain close to the diagonal, indicating acceptable results (Fig. 4E). The Hosmer-Lemeshow test yields a p-value of 0.944 in the training set and 0.425 in the external validation set, indicating the adequacy of fit of the nomograms in both sets. Furthermore, there is no

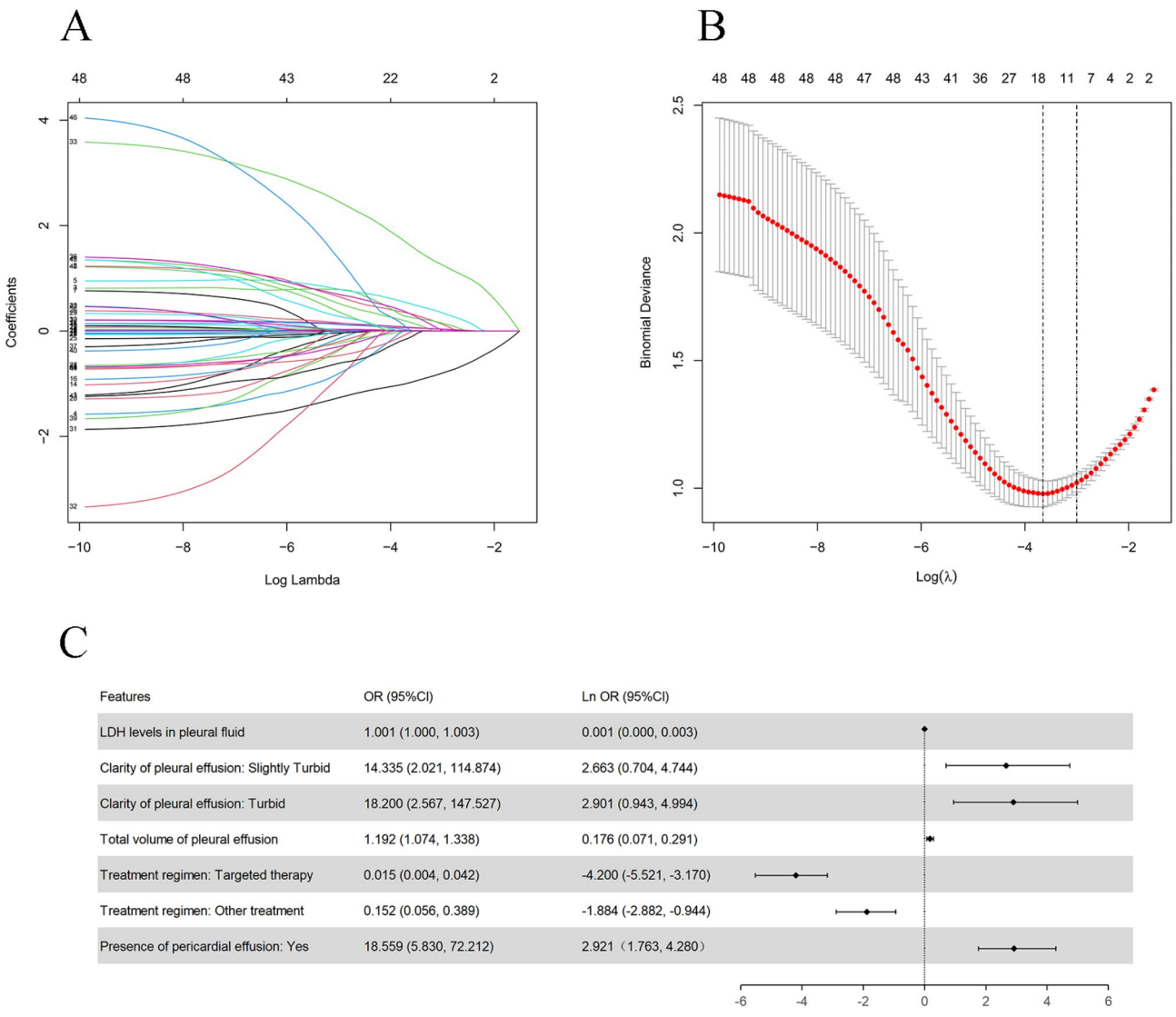

Fig. 2 Selection of clinical features. **A**-**B**: The optimal parameter (lambda) selection in the LASSO was performed through tenfold cross-validation, resulting in the selection of the optimal lambda value of 0.0259. This choice led to 17 features with nonzero coefficients. **C**: Further screening of clinical features using logistic regression and plotting their Odds Ratio (OR) in a forest plot. Note: The OR of continuous variables indicates the multiplicative change in the probability of an event occurring with each unit increase

significant difference between the predicted values and the actual values. Finally, DCA of the nomogram in both the training set (Fig. 4F) and the external validation set (Fig. 4G) underscored the significant clinical benefits of utilizing the nomogram for early intervention in patients with MPE at the time of initial diagnosis of lung cancer.

Utilizing the nomogram to predict prognosis across different pathological types of lung cancer and stratifying patient risk accordingly

To assess the prognostic efficacy of the nomogram across various pathological types of lung cancer, a subgroup analysis was conducted on the 228 patients in the training set. The results (Fig. 5A) unveiled that the nomogram's predictive accuracy for patients with lung adenocarcinoma (LUAD) stood at 87.3%, boasting a specificity of 84.2% and a sensitivity of 91.0%. For patients with lung squamous cell carcinoma (LUSC), the predictive accuracy reached 92.9%, with a specificity of 85.7% and a sensitivity of 95.2%. Conversely, for those diagnosed with small cell lung cancer (SCLC), the predictive accuracy, specificity, and sensitivity were recorded at 81.5%, 75.0%, and 84.2%. Subsequent to this analysis, risk scoring was conducted on the patients in the training set based on nomograms, yielding three cutoff values: (1) a risk score corresponding to the highest sensitivity; (2) a risk score corresponding to the maximum sensitivity + specificity; (3) a risk score corresponding to the maximum specificity. Following this, patients were categorized into four risk groups: a low-risk group (< 75

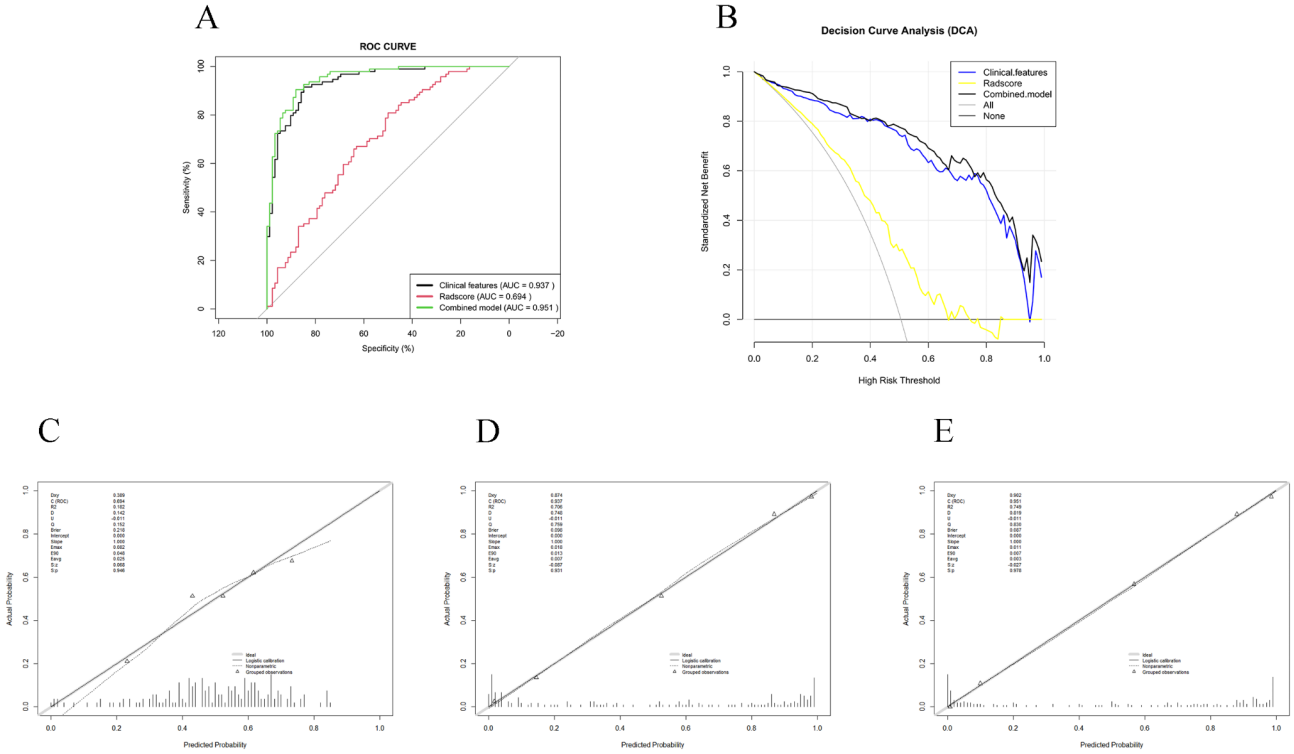

Fig. 3 Comparison of different model performances. **A**: ROC curves for the clinical features model, radscore model, and combined model; **B**: DCA for the clinical features model, radscore model, and combined model. The threshold probability for the clinical features model ranges from 0.01 to 0.95, for the radscore model it ranges from 0.01 to 0.66, and for the combined model it ranges from 0.01 to 1.00; **C**: Calibration curves for the radscore model; **D**: Calibration curves for the clinical features model; **E**. Calibration curves for the combined model

points), a medium-risk group (75–115 points), a high-risk group (115–166 points), and a very high-risk group (≥ 166 points).

After risk stratification of all patients in both the training and external validation sets based on risk scores (Fig. 5B), the analysis unveiled 39 patients in the low-risk group, all of whom survived with a 0% mortality rate within one year. In the medium-risk group, consisting of 81 patients, 67 survived while 14 succumbed to mortality after one year, equating to a 17.28% mortality rate. The high-risk group encompassed 122 patients, with 27 surviving and 95 experiencing mortality within one year, resulting in a mortality rate of 77.87%. Finally, the very high-risk group comprised 65 patients, all of whom succumbed to mortality within one year, accounting for a 100% mortality rate. The overall survival (OS) of patients in different subgroups demonstrates a spectrum of prognostic outcomes ranging from favorable to unfavorable across the low-risk, intermediate-risk, high-risk, and very high-risk groups (Fig. 5C). The median survival times for patients in these groups were 26 months (95% CI: 22.339–29.671), 21 months (95% CI: 18.599–23.401), 9 months (7.873–10.127), and 2 months (95% CI: 1.368–2.632), respectively.

Discussion

The treatment of lung cancer with MPE involves both systemic and local therapies. Systemic therapy aims to alleviate MPE by treating the primary lung cancer lesion and remains the cornerstone of treatment. In contrast, local therapy primarily addresses symptom relief and enhances the patient's quality of life. For patients with severe symptoms and extensive MPE, local therapy is generally recommended as the first line of treatment to alleviate discomfort.

Current local treatment options for lung cancer with MPE include therapeutic thoracentesis, indwelling pleural catheter, pleurodesis, intrapleural chemotherapy, intrapleural chemotherapy combined with anti-angiogenic agents, hyperthermic intrathoracic chemotherapy, and video-assisted thoracoscopic surgery. Indwelling pleural catheter is the preferred approach but can lead to complications such as infection, catheter-related metastasis, and catheter obstruction [11, 12]. Repeated thoracentesis can effectively relieve symptoms, but it may increase the frequency of hospitalization and the risk of complications [13–15].

Pleurodesis promotes pleural adhesion using sclerosing agents to prevent fluid re-accumulation but may also cause infection or acute respiratory distress syndrome [16, 17]. Intrapleural chemotherapy directly targets the

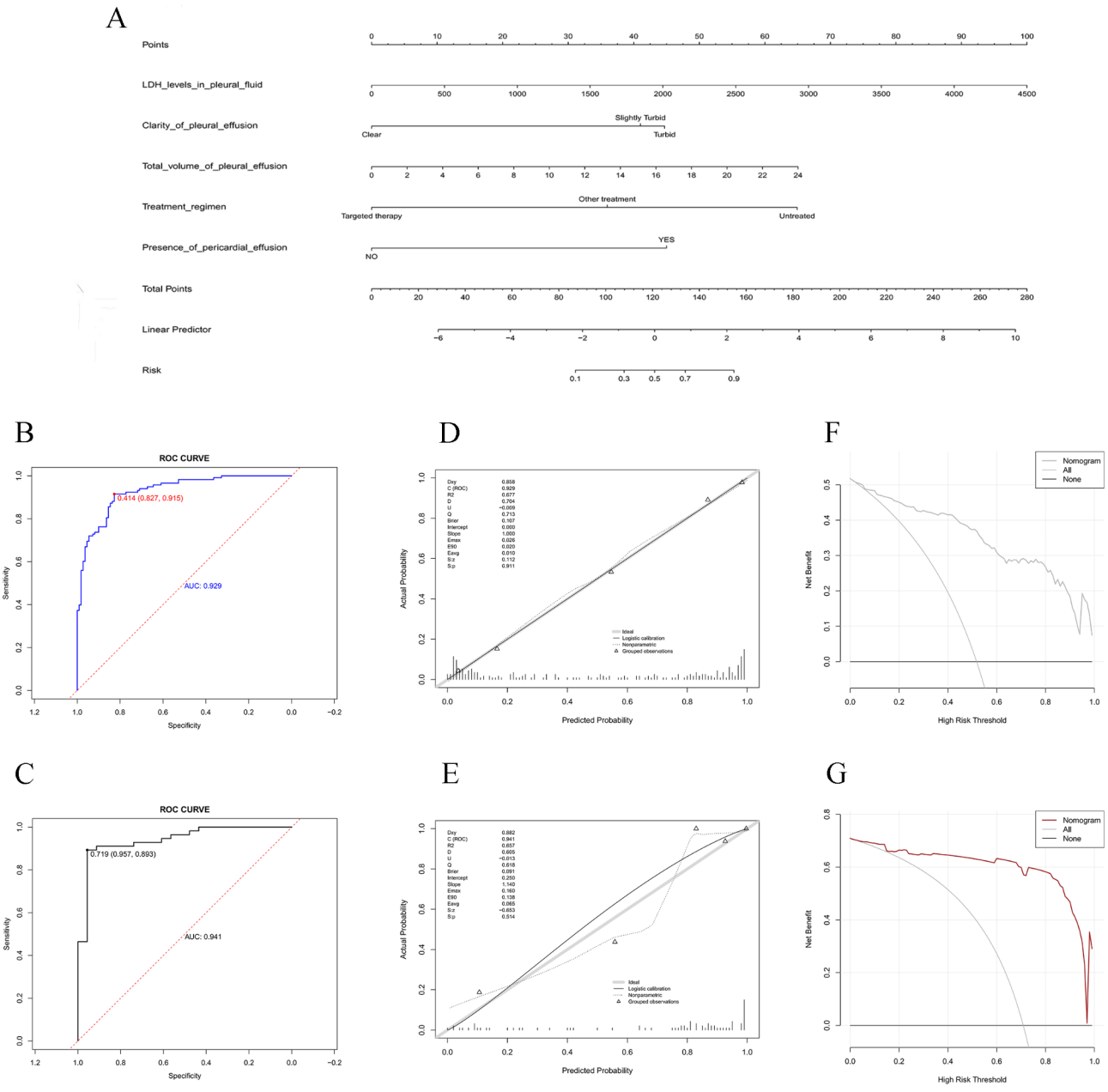

Fig. 4 Establishment and validation of the nomogram. **A**: A nomogram formulated utilizing 5 predictive factors; **B**: ROC curves of the nomogram in the modeling group and external validation group; **C**-**D**: Calibration curves of the nomogram in the modeling group and external validation group; **E**-**F**: Clinical decision curves of the nomogram in the modeling group and external validation group. The threshold probability in the modeling group ranges from 0.01 to 1.00, and in the external validation group, it ranges from 0.02 to 1.00

Table 1 The AUCs and corresponding sensitivity and specificity of the nomogram

Goup	AUC	Sensitivity	Specificity	PPV	NPV	Accuracy
Training set	0.929 (0.897–0.960)	0.915 (0.865–0.966)	0.827 (0.757–0.898)	0.850 (0.788–0.912)	0.901 (0.843–0.959)	0.873 (0.872–0.874)
Validation set	0.941 (0.885–0.997)	0.893 (0.812–0.974)	0.957 (0.873-1.000)	`0.980 (0.942-1.000)	0.786 (0.634–0.938)	0.911 (0.909–0.913)

Note: Data are shown as percentage (95% confidence interval)

Abbreviations: AUC, area under the receiver-operating-characteristic curve; NPV, negative predictive value; PPV, positive predictive value

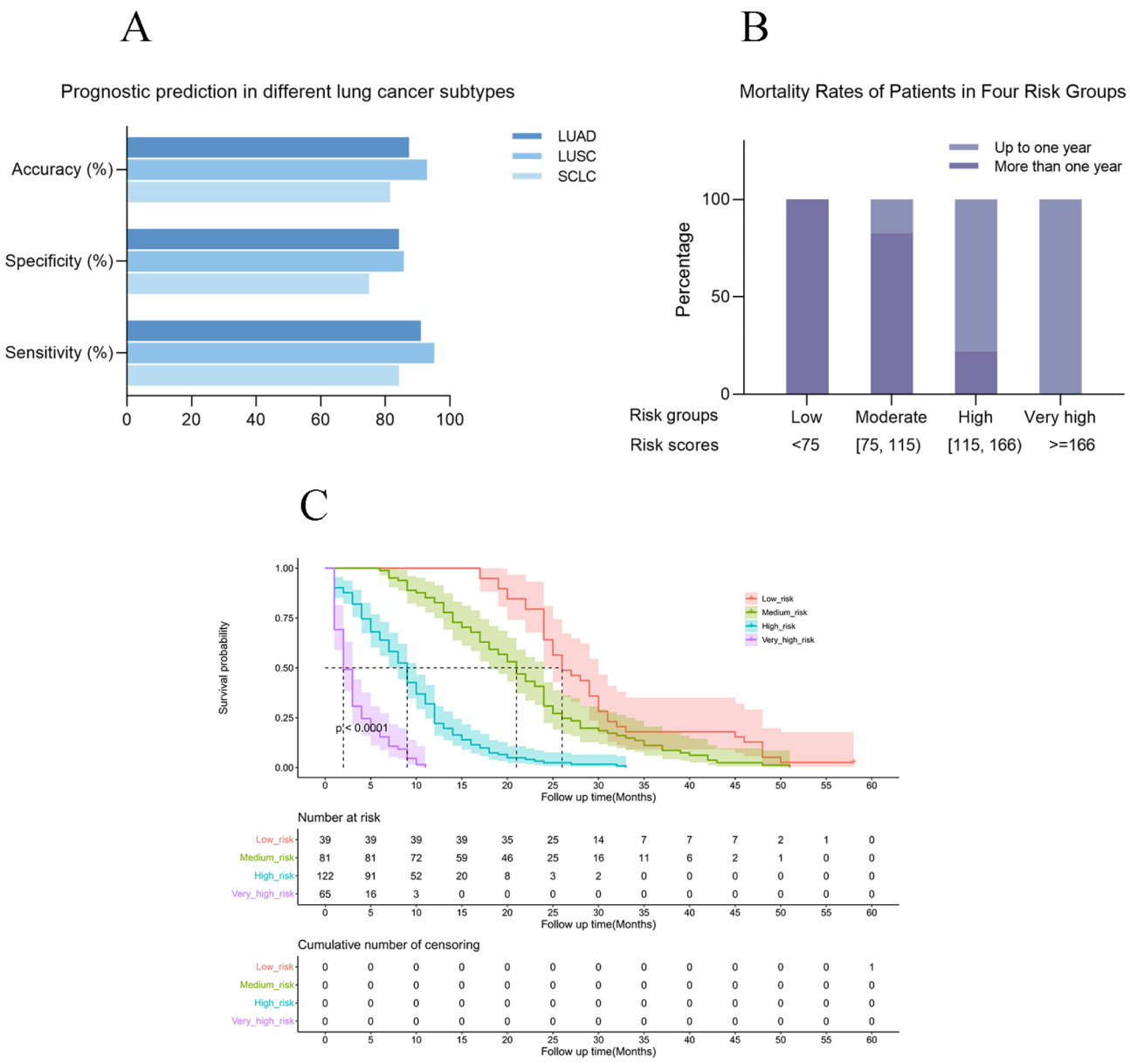

Fig. 5 Predictive performance of the nomogram for prognosis of different lung cancer types and patient risk stratification. **A**: Predictive performance of the nomogram for adenocarcinoma, squamous cell carcinoma, and small cell lung cancer. **B**: Distribution of deceased and surviving patients among four risk groups: low, moderate, high, and very high risk. Scores less than 75 points represent the low-risk group, 75–115 points (excluding 115 points) represent the moderate-risk group, 115–166 points represent the high-risk group (excluding 166 points), and scores greater than or equal to 116 points represent the very high-risk group. **C**: Prognosis of patients in the four risk groups

tumor, providing local anti-tumor effects. However, platinum-based drugs have notable side effects in patients with advanced lung cancer, often requiring combination therapy with other drugs to mitigate toxicity and enhance efficacy [18]. A meta-analysis revealed that platinum-based chemotherapy combined with recombinant human vascular endothelial growth factor inhibitors significantly improved the objective response rate, disease control rate, and quality of life, outperforming single-agent lobaplatin treatment [19]. Another study indicated that combining bevacizumab with cisplatin for intrapleural therapy in non-squamous non-small cell lung cancer with MPE markedly improved the effective rate and progression-free survival, both of which were significantly better than cisplatin monotherapy [20].

Recent studies have suggested that nocadia rubra cell wall skeleton preparation and IL-2 are effective regulators for MPE treatment, enhancing immune responses and inhibiting tumor growth [21, 22]. However, therapies such as hyperthermic intrathoracic chemotherapy and video-assisted thoracoscopic surgery still require further validation through large-scale, multi-center

clinical trials to assess their effectiveness and safety more comprehensively.

Despite the wide range of available local treatments, there is currently no clear evidence indicating that one method is superior to the others. As such, early prognosis assessment and individualized treatment strategies remain crucial for improving treatment outcomes.

In this retrospective analysis, a clinical features model with LDH levels in pleural fluid, clarity of pleural effusion, treatment regimen, presence of pericardial effusion, and total volume of pleural effusion forecasted MPE prognosis at lung cancer diagnosis. Incorporating imaging data minimally enhanced predictive capability, leading to constructing a nomogram based solely on these clinical parameters. The developed nomograms accurately predicted MPE prognosis at lung cancer diagnosis. The training set's nomogram had an AUC of 0.929 (95% CI: 0.897–0.961), with satisfactory calibration curve concordance. The external validation set's nomogram had an AUC of 0.941 (95% CI: 0.885–0.997), though less robust calibration curves, possibly due to limited external validation cohort size. Nonetheless, nomograms performed well in both sets in clinical decision curves. Scoring and stratifying patients by risk, scores < 75 were low risk, 75–115 medium, 115–166 high, and ≥ 166 very high. This method effectively predicted one-year mortality, with significant prognosis differences across risk groups.

The LENT scoring system was developed to predict the prognosis of patients with MPE at various time points. External validation of the system reported AUC values of 0.78, 0.76, and 0.81 for 1-month, 3-month, and 6-month outcomes, respectively [23]. The target population for this scoring system is broad, as it applies to all patients with malignant pleural effusion. Another study developed a nomogram model specifically for predicting the 12-month survival of lung cancer patients with malignant pleural effusion or pericardial effusion. This model achieved an AUC of 0.766 in an external validation cohort, which is superior to the 0.677 AUC reported by the LENT scoring system [24].

In our study, we further refined the study population by narrowing the inclusion criteria, resulting in a more specific cohort. By incorporating a broader range of clinical, laboratory, and imaging factors, we developed a more accurate nomogram. Although our external validation cohort consists of a different population compared to those in prior studies, the nomogram achieved an AUC of 0.941 in our external validation cohort, which is significantly higher than the AUCs reported in previous research, even surpassing the AUC observed in their internal validation.

Despite the nomogram's robust predictive performance, study limitations exist, like lacking data segmentation for internal validation due to limited patient numbers. However, external validation data from 79 patients showed excellent performance, reducing internal validation necessity. Nonetheless, additional center data validation is crucial. Furthermore, we opted for 2D ROI delineation. While this method is straightforward to implement, its main limitation lies in its inability to fully capture the three-dimensional morphology of tumors. Consequently, this may lead to an incomplete assessment of tumor size, shape, and growth trajectory.

Another limitation of our study is the absence of data on lung cancer patients treated with immunotherapy. While we attempted to include this group, the patients who received immunotherapy were unfortunately lost to follow-up. Given the increasing use of immunotherapy in clinical practice, our predictive model may not be fully applicable to this patient group. This underscores the importance of including immunotherapy-treated patients in future studies to ensure a more comprehensive validation of the model.

Conclusion

This study introduces a clinical features-based nomogram for MPE prognostic assessment at lung cancer diagnosis. It holds promise for early prognosis determination, aiding prompt intervention for patients with poor prognoses.

Abbreviations

MPE	Malignant pleural effusion
LASSO	Least absolute shrinkage and selection operator
ROC	Receiver operating characteristic
AUC	Area under the curve
DCA	Decision curve analysis
LDH	Lactate dehydrogenase
CT	Computed tomography
PET-CT	Positron emission tomography-computed tomography
MRI	Magnetic resonance imaging
ROI	Region of interest
NPV	Negative predictive value
PPV	Positive predictive value
CI	Confidence interval
OS	Overall survival
LUAD	Lung adenocarcinoma
LUSC	Lung squamous cell carcinoma
SCLC	Small cell lung cancer
OR	Odds ratio

Supplementary Information

The online version contains supplementary material available at https://doi.org/10.1186/s12885-025-13632-z .

Supplementary Material 1

Acknowledgements

None.

Author contributions

YJ: Conceptualized and designed the study, performed data analysis and statistical analysis, and drafted the manuscript.XH: Equally contributed to the study design, acquired data, conducted statistical analysis, and contributed to manuscript preparation and editing.YH: Contributed to data acquisition

and assisted in manuscript preparation and editing.HW: Assisted in data acquisition and participated in manuscript preparation and editing.TD: Contributed to data acquisition and assisted in manuscript preparation and editing.LJ: Conceived the study, supervised the entire research process, directed the literature search, oversaw data analysis and statistical analysis, prepared and edited the manuscript, and served as the primary contact for communications with the journal and other authors.

Funding
This work was supported by the Scientific Research Development Fund of North Sichuan Medical College (CBY23-QNA47).

Data availability
The datasets that were either generated or analyzed during the current study are made available by the corresponding author upon receipt of a reasonable request.

Declarations

Ethics approval and consent to participate
The study was approved by the Medical Ethics Committee of Affiliated Hospital of North Sichuan Medical College with file number 2023ER423-1. Informed consent was waived due to the retrospective nature of the study, where data was sourced from the hospital's electronic medical records and electronic health check databases. The study met the following conditions for consent waiver: (1) The risk to subjects was no more than minimal; (2) The waiver did not adversely affect the rights and welfare of the subjects; (3) The research involved identifiable private information that could not feasibly be obtained otherwise, and did not involve personal privacy or commercial interests; (4) The study posed no harm or additional costs to the patients, and the data obtained could contribute to medical advancements for similar conditions; (5) The waiver of informed consent was approved by the ethics committee and did not imply exemption from ethical review.

Consent for publication
Not applicable.

Competing interests
The authors declare no competing interests.

Received: 13 May 2024 / Accepted: 3 February 2025
Published online: 10 February 2025

References

1. Feller-Kopman DJ, Reddy CB, DeCamp MM, Diekemper RL, Gould MK, Henry T, Iyer NP, Lee Y, Lewis SZ, Maskell NA, et al. Management of malignant pleural effusions. An official ATS/STS/STR clinical practice Guideline. Am J Respir Crit Care Med. 2018;198(7):839–49.
2. Porcel JM, Gasol A, Bielsa S, Civit C, Light RW, Salud A. Clinical features and survival of lung cancer patients with pleural effusions. Respirology. 2015;20(4):654–9.
3. Psallidas I, Kalomenidis I, Porcel JM, Robinson BW, Stathopoulos GT. Malignant pleural effusion: from bench to bedside. Eur Respir Rev. 2016;25(140):189–98.
4. Ferreiro L, Toubes ME, San JM, Suarez-Antelo J, Golpe A, Valdes L. Advances in pleural effusion diagnostics. Expert Rev Respir Med. 2020;14(1):51–66.
5. Taghizadeh N, Fortin M, Tremblay A. US hospitalizations for malignant pleural effusions: data from the 2012 National Inpatient Sample. Chest. 2017;151(4):845–54.
6. Peng P, Yang Y, Du J, Zhai K, Shi HZ. Prognostic biomarkers of malignant patients with pleural effusion: a systematic review and meta-analysis. CANCER CELL INT. 2022;22(1):99.
7. Wyld L, Audisio RA, Poston GJ. The evolution of cancer surgery and future perspectives. NAT REV CLIN ONCOL. 2015;12(2):115–24.
8. Schaue D, McBride WH. Opportunities and challenges of radiotherapy for treating cancer. NAT REV CLIN ONCOL. 2015;12(9):527–40.
9. Baudino TA. Targeted Cancer Therapy: the Next Generation of Cancer Treatment. Curr Drug Discov Technol. 2015;12(1):3–20.
10. MacMahon H, Naidich DP, Goo JM, Lee KS, Leung A, Mayo JR, Mehta AC, Ohno Y, Powell CA, Prokop M et al. Guidelines for Management of Incidental Pulmonary Nodules Detected on CT Images: From the Fleischner Society 2017. RADIOLOGY: 2017, 284(1):228–243.
11. Tremblay A, Michaud G. Single-center experience with 250 tunnelled pleural catheter insertions for malignant pleural effusion. Chest. 2006;129(2):362–8.
12. Davies HE, Mishra EK, Kahan BC, Wrightson JM, Stanton AE, Guhan A, Davies CW, Grayez J, Harrison R, Prasad A, et al. Effect of an indwelling pleural catheter vs chest tube and talc pleurodesis for relieving dyspnea in patients with malignant pleural effusion: the TIME2 randomized controlled trial. JAMA-J AM MED ASSOC. 2012;307(22):2383–9.
13. Feller-Kopman D, Light R. Pleural Disease. NEW ENGL J MED. 2018;378(8):740–51.
14. Roberts ME, Neville E, Berrisford RG, Antunes G, Ali NJ. Management of a malignant pleural effusion: British thoracic Society Pleural Disease Guideline 2010. Thorax. 2010;65(Suppl 2):ii32–40.
15. Antony VB, Loddenkemper R, Astoul P, Boutin C, Goldstraw P, Hott J, Rodriguez PF, Sahn SA. Management of malignant pleural effusions. EUR RESPIR J. 2001;18(2):402–19.
16. Hughes SM, Carmichael JJ. Malignant pleural effusions: updates in diagnosis and management. LIFE-BASEL 2022, 13(1).
17. Janssen JP, Collier G, Astoul P, Tassi GF, Noppen M, Rodriguez-Panadero F, Loddenkemper R, Herth FJ, Gasparini S, Marquette CH, et al. Safety of pleurodesis with talc poudrage in malignant pleural effusion: a prospective cohort study. Lancet. 2007;369(9572):1535–9.
18. Zhao WY, Chen DY, Chen JH, Ji ZN. Effects of intracavitary administration of Endostar combined with cisplatin in malignant pleural effusion and ascites. CELL BIOCHEM BIOPHYS. 2014;70(1):623–8.
19. Wang CQ, Liu FY, Wang W. Thoracic perfusion of lobaplatin combined with endostar for treating malignant pleural effusions: a meta-analysis and systematic review. Medicine. 2022;101(40):e30749.
20. Du N, Li X, Li F, Zhao H, Fan Z, Ma J, Fu Y, Kang H. Intrapleural combination therapy with bevacizumab and cisplatin for non-small cell lung cancer–mediated malignant pleural effusion. ONCOL REP. 2013;29(6):2332–40.
21. Wu J, He B, Miao M, Han X, Dai H, Dou H, Li Y, Zhang X, Wang G. Enhancing natural killer cell-mediated Cancer Immunotherapy by the Biological Macromolecule Nocardia Rubra Cell-Wall Skeleton. PATHOL ONCOL RES. 2022;28:1610555.
22. Meng Y, Sun J, Wang X, Ma Y, Kong C, Zhang G, Dou H, Nan N, Shi M, Yu T, et al. The biological macromolecule Nocardia Rubra cell-wall skeleton as an avenue for cell-based immunotherapy. J CELL PHYSIOL. 2019;234(9):15342–56.
23. Clive AO, Kahan BC, Hooper CE, Bhatnagar R, Morley AJ, Zahan-Evans N, Bintcliffe OJ, Boshuizen RC, Fysh ET, Tobin CL, et al. Predicting survival in malignant pleural effusion: development and validation of the LENT prognostic score. Thorax. 2014;69(12):1098–104.
24. Tian T, Zhang P, Zhong F, Sun C, Zhou J, Hu W. Nomogram construction for predicting survival of patients with non-small cell lung cancer with malignant pleural or pericardial effusion based on SEER analysis of 10,268 patients. ONCOL LETT. 2020;19(1):449–59.

Publisher's note

Springer Nature remains neutral with regard to jurisdictional claims in published maps and institutional affiliations.